Novel Tools and Methods

Oral and Injected Tamoxifen Alter Adult Hippocampal Neurogenesis in Female and Male Mice

Bryon M. Smith,[1] Angela I. Saulsbery,[1] Patricia Sarchet,[1] Nidhi Devasthali,[1] Dalia Einstein,[1] and Elizabeth D. Kirby[1,2]
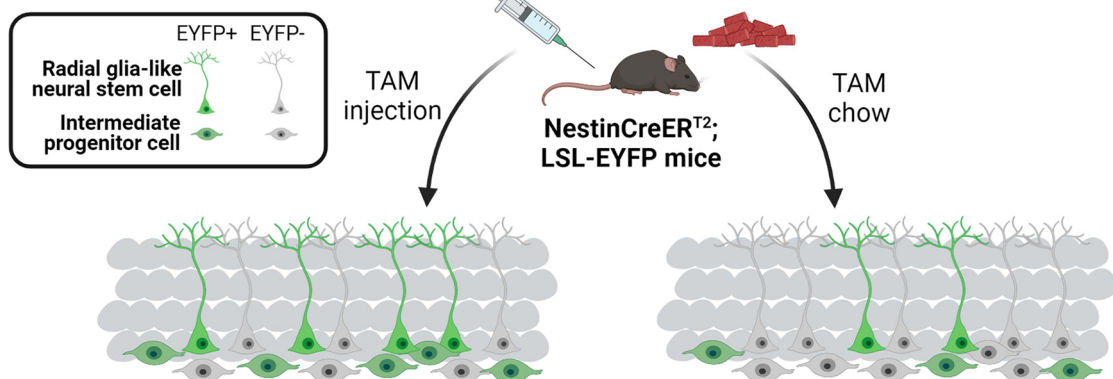
https://doi.org/10.1523/ENEURO.0422-21.2022

[1]Department of Psychology, College of Arts and Sciences, The Ohio State University, Columbus, OH 43210 and [2]Chronic Brain Injury Initiative, The Ohio State University, Columbus, OH 43210

Visual Abstract
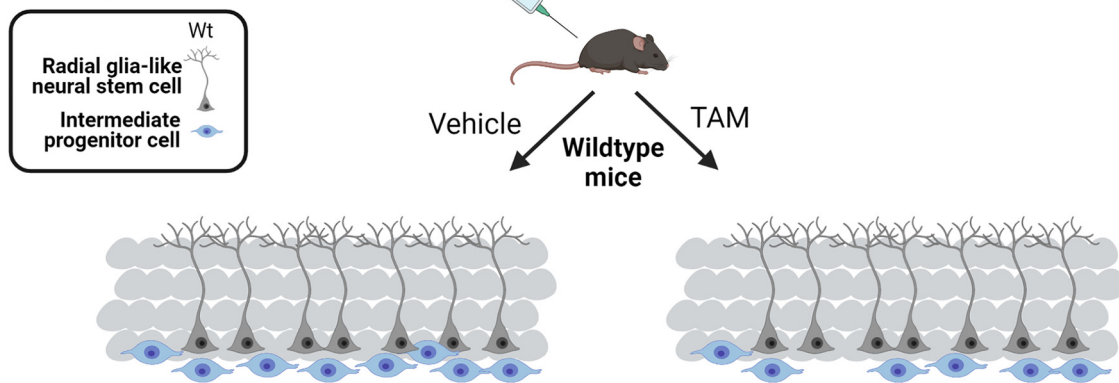
Significance Statement

Numerous transgenic mouse models use the inducible Cre-Lox system in which a synthetic estrogen tamoxifen (TAM) is used to initiate recombination of genetic sequences flanked by LoxP sites. Despite widespread use, there is little data available about the effectiveness of different TAM delivery methods. Here, we show that giving adult mice in which inducible Cre is expressed in neural stem and progenitor cells (NSPCs) TAM via injection (the most commonly-used route) and chow both induce recombination in those target cells. However, chow delivery is far less efficient than injections and both delivery methods alter adult neurogenesis on their own when compared with vehicle-treated mice. These findings provide guidance for investigators choosing experimental design with inducible Cre systems.

Inducible Cre recombinase facilitates temporal control of genetic recombination in numerous transgenic model systems, a feature which has made it a popular tool for adult neurogenesis studies. One of the most common forms of inducible Cre, CreER^{T2}, requires activation by the selective estrogen receptor modulator tamoxifen (TAM) to initiate recombination of LoxP-flanked sequences. To date, most studies deliver TAM via intraperitoneal injection. But the introduction of TAM-infused commercial chows has recently expanded the possible modes of TAM delivery. Despite the widespread use of TAM-inducible genetic models in adult neurogenesis research, the comparative efficiency and off-target effects of TAM administration protocols is surprisingly infrequently studied. Here, we compare a standard, 5 d TAM injection regimen with voluntary consumption of TAM-infused chow. First, we used adult NestinCreER^{T2};Rosa-LoxP-STOP-LoxP-EYFP reporter mice to show that two weeks of TAM chow and 5 d of injections led to LoxP recombination in a similar phenotypic population of neural stem and progenitor cells (NSPCs) in the adult dentate gyrus. However, TAM chow resulted in substantially less overall recombination than injections. TAM administration also altered adult neurogenesis, but in different ways depending on administration route: TAM injection disrupted neural progenitor cell proliferation three weeks after TAM, whereas TAM chow increased neuronal differentiation of cells generated during the diet period. These findings provide guidance for selection of TAM administration route and appropriate controls in adult neurogenesis studies using TAM-inducible Cre mice. They also highlight the need for better understanding of off-target effects of TAM in other neurologic processes and organ systems.

Key words: adult neurogenesis; hippocampal neurogenesis; hippocampus; inducible Cre recombinase; neurogenesis; tamoxifen

Introduction

Adult neurogenesis is a widely conserved process among mammalian species in which resident neural stem cells generate new neurons that integrate into mature circuitry throughout the lifespan. Evidence that neurogenesis in the adult rodent dentate gyrus of the hippocampus supports memory and affect regulation has spurred interest in both its natural functions across species, as well as its potential therapeutic applications in humans (for

review, see McAvoy and Sahay, 2017; Miller and Sahay, 2019; Toda et al., 2019).

The study of time-specific and tissue-specific phenomena, such as adult hippocampal neurogenesis, has been accelerated by the introduction of several inducible methods of gene expression manipulation. Tamoxifen (TAM)-inducible Cre mouse lines (e.g., CreER^{T2}) have proven to be particularly valuable tools for inducible manipulation of gene expression in the adult neurogenic lineage. In these models, Cre recombinase is fused to a mutated estrogen receptor (ER^{T2}) which retains Cre in the cytoplasm until the receptor binds its ligand, the selective estrogen receptor modulator TAM (Feil et al., 1997; Danielian et al., 1998). TAM binding allows translocation of the mutated estrogen receptor and its fused Cre enzyme to the nucleus, where Cre can induce recombination of LoxP-flanked genetic sequences. Use of a tissue-specific promoter can further constrain CreER^{T2} expression to specific cell classes. For example, neural stem and progenitor cells (NSPCs) are commonly targeted using GLAST, Nestin, SOX2, or GFAP promoters (to name a few common versions; Semerci and Maletic-Savatic, 2016).

In adult neurogenesis studies using CreER^{T2}-mediated LoxP recombination, two dominant approaches to selecting controls have emerged. One approach compares

mice of different genotypes (Cre+/− or LoxP+/−), all of which are treated with TAM. A second approach is to compare mice of the same genotype treated with TAM versus those treated with vehicle. This latter comparison is predicated on TAM itself being inert, aside from its ability to induce CreER^{T2} translocation. Yet, gonadal steroid hormones, including estrogens, can modulate brain processes such as neurogenesis and cell survival (Jorgensen and Wang, 2020).

The effect of TAM on adult neurogenesis is generally understudied and the few existing studies have yielded mixed results. For example, Rotheneichner et al. (2017) found no inherent effects of TAM on cell proliferation and fate in the dentate gyrus of the adult mouse hippocampus, but a more recent study suggested long-lasting suppression of hippocampal cell proliferation in juvenile mice (Lee et al., 2020). Given the widespread use of TAM-inducible models in adult neurogenesis, it is imperative to understand how TAM itself (independent of transgene expression) affects adult neurogenic processes.

Beyond the selection of controls, TAM administration route is another important potential design variable in studies using CreER^{T2} mouse models. Intraperitoneal injections are by far the most common method of exposing mice to TAM in adult neurogenesis studies to date. However, administration of TAM through voluntary consumption of custom laboratory chow is a promising alternative that might reduce injection-related stress and researcher hands-on time. TAM-infused chows have been used successfully in cardiac research (Kiermayer et al., 2007), and may be applicable to other adult tissues as well (Yoshinobu et al., 2021). It is unknown how TAM chow compares to TAM injection as regards recombination efficiency and appropriate dosing schedules for adult neurogenesis research.

Here, we compare TAM administration by injection and chow, both in terms of the specificity and efficiency of LoxP recombination and the inherent effects of TAM treatment itself on adult neurogenesis. Using a CreER^{T2} model targeted to NSPCs by a Nestin promoter, our findings suggest that TAM chow can induce LoxP recombination in hippocampal NSPCs with similar specificity as TAM injection, but that TAM chow results in much lower recombination efficiency than injections, likely because of chow avoidance and therefore lower TAM exposure. We also show that both TAM injection and TAM chow paradigms have inherent, although different, effects on adult neurogenesis, underscoring the need to compare TAM-treated experimental animals to genetic controls similarly treated with TAM, regardless of route of administration.

Materials and Methods

Mice

All mice were group housed with three to five mice per cage in The Ohio State University Psychology building mouse vivarium in standard ventilated cages on a 12/12 h light/dark cycle (lights on 6:30 A.M.) with *ad libitum* access to food and water. Male and female mice were eight to nine weeks old at the time of the experiment and housed in groups of two to four. All animal use was in accordance with institutional guidelines approved by The Ohio State University Institutional Animal Care and Use Committee.

Experimental design and statistical analysis

Study 1: TAM injection versus TAM chow

Seven- to nine-week-old NestinCreER^{T2} (Lagace et al., 2007; Jackson #016261); R26R-LoxP-STOP-LoxP-EYFP (Srinivas et al., 2001; Jackson #007909) littermates were randomly assigned by whole cage to one of four groups: TAM inject d(day)7 perfuse ($n = 10$), TAM inject d14 perfuse ($n = 11$), TAM chow 10 d ($n = 7$), TAM chow 14 d ($n = 11$). Mice were bred by crossing wild-type C57Bl/6J mice with mice homozygous for both NestinCreER^{T2} and R26R-LoxP-STOP-LoxP-EYFP; thus, offspring were heterozygous for both transgenes. TAM-injected mice received daily 180 mg/kg/d intraperitoneal injections of TAM for 5 d. TAM chow mice were first acclimated to standard chow provision in a dish on the cage floor for 3 d before switching to TAM chow. Food was weighed and refreshed every 2–4 d. At the indicated tissue harvest time, mice were anesthetized with an 87.5 mg/kg ketamine, 12.5 mg/kg xylazine mixture, and then transcardially perfused with ice-cold 0.1 M PBS. Body weight data were analyzed by a repeated measures mixed-effects model (day × TAM) within each sex, followed by Sidak's multiple comparisons within day. This analysis was performed within sex individually to prevent the strong main effect of sex on body weight from masking any more subtle effects of TAM. Food consumption was analyzed by two-way ANOVA (sex × day) followed by Sidak's multiple comparisons between days within sex. Cell count data were analyzed by one-way ANOVA followed by Tukey's *post hoc* tests or by two-way ANOVA (hippocampal subregion × group) followed by Tukey's *post hoc* multiple comparisons between groups within subregion.

Study 2: TAM versus vehicle injection

Wild-type C57Bl6/J mice were obtained at six weeks of age from The Jackson Laboratory (#000664) and allowed to acclimate for two weeks. Cages of mice were randomly assigned to either TAM ($n = 11$ mice) or vehicle (sunflower oil, $n = 12$ mice) injection groups. TAM injections were as described for study 1. On the last 3 d of TAM/vehicle injection, mice also all received daily bromodeoxyuridine (BrdU) injections (150 mg/kg/d, i.p.). Twenty-one days after the last TAM/BrdU injections, mice received a single injection of ethynyldeoxyuridine (EdU; 150 mg/kg, i.p.) and were perfused as in Study 1 2 h later. Body weight data were analyzed by a repeated measures mixed-effects model (day × TAM) within each sex, followed by Sidak's multiple comparisons within day. BrdU+/EdU+ density was compared by unpaired *t* test. Density and proportion of BrdU/DCX/NeuN or EdU/GFAP/SOX2 cell subtypes was compared by two-way repeated measures ANOVA followed by *post hoc* Sidak's multiple comparisons within cell type.

Table 1: Antibodies used

Primary antibody	Vendor/product number	RRID	Dilution	Secondary	Vendor/product number	Dilution	RRID
Rabbit anti-GFP	ThermoFisher A11122	AB_221569	1:1000	Donkey Alexa Fluor 488 anti-rabbit	Fisher A21206	1:500	AB_2535792
Mouse anti-GFAP	EMD Millipore MAB360	AB_11212597	1:1000	Donkey Alexa Fluor 647 anti-mouse	Fisher A31571	1:500	AB_162542
Rat anti-SOX2	Affymetrix eBioscience 14–9811	AB_11219471	1:1000	Donkey Alexa Fluor 594 anti-rat	Fisher A21209	1:500	AB_2535795
Rabbit anti-DCX	Cell Signaling 4604	AB_561007	1:500	Donkey Alexa Fluor 555 anti-rabbit	Fisher A31572	1:500	AB_162543
Mouse anti-NeuN	EMD Millipore MAB377	AB_2298772	1:1000	Donkey Alexa Fluor 647 anti-mouse	Fisher A31571	1:500	AB_162542
Rat anti-BrdU	Bio-Rad OBT0030	AB_609568	1:500	Donkey Alexa Fluor 488 anti-mouse	Fisher A21202	1:500	AB_141607

List of primary and secondary antibodies.

Study 3: TAM versus vehicle chow

Wild-type C57Bl6/J mice were obtained at six weeks of age from The Jackson Laboratory (#000664) and allowed to acclimate for one week. Cages of mice were randomly assigned to either TAM ($n = 11$ mice) or vehicle ($n = 12$ mice) chow groups. Diet was provided as described for Study 1 for 14 d. On the last 3 d of TAM/vehicle chow, mice also all received daily BrdU injections (150 mg/kg/d, i.p.). 21 d after the last TAM/BrdU injections, mice received a single injection of EdU (150 mg/kg, i.p.) and were perfused as in Study 1 2 h later. Food consumption was analyzed by repeated measures two-way ANOVA (chow type × day) followed by Sidak's multiple comparisons between chow type within days. Remaining analysis for this experiment is similar to that for Study 2.

TAM injection preparation

TAM (Fisher #50-115-2413) was dissolved overnight at 20 mg/ml at 37°C in sterile sunflower oil then stored at +4°C for one week maximum, all while protected from light. Cumulative TAM dose for each mouse was calculated by adding the mg of TAM in each injection over the 5 d of the dosing schedule.

TAM and vehicle chow

TAM chow (500 mg TAM/kg diet, TD.130858, also contains 49.5 g/kg sucrose; 15.4% protein, 55.1% carbohydrate, and 3.4% fat by weight; and 0.25 g/kg of red food color) and matched vehicle chow (15.4% protein, 55.1% carbohydrate, and 3.4% fat by weight; 50 g/kg of sucrose; and 0.25 g/kg of blue food color) were obtained from Envigo and stored at +4°C in the dark until given to mice. Chow was refreshed every 3 d per manufacturer recommendations.

BrdU and EdU preparation

BrdU (Sigma, #B5002) and EdU (Click Chemistry Tools, #1149-500) were each dissolved fresh in sterile physiological saline at 10 mg/ml.

Tissue processing

Tissue fixation, slicing, and immunofluorescent staining were performed similarly to our previous work (Dause and Kirby, 2020) using the antibodies described in Table 1. In brief, brains were postfixed in 4% paraformaldehyde (Fisher #AC169650010) in 0.1 M phosphate buffer at +4°C for 24 h then equilibrated in 30% sucrose (Fisher S5-3) in 0.1 M PBS (Fisher #BP399-20) at +4°C before slicing on a freezing microtome (Leica) in a 1:12 series of 40-μm-thick coronal sections. Sections were stored in cryoprotectant medium at −20°C until processed for immunofluorescent staining. Free-floating sections were rinsed in PBS, blocked in 1% normal donkey serum (Jackson ImmunoResearch #017000121), 0.3% Triton X-100 (Fisher #AC215682500) in PBS and incubated in primary antibody in blocking solution overnight at 4°C on rotation. The next day, sections were rinsed, incubated in secondary antibody in blocking solution for 2 h at room temperature on rotation and then rinsed and counterstained with Hoechst 33342 (1:2000 in PBS, Fisher #H3570) before being mounted on SuperFrost Plus slides (Fisher #12-550-15), dried and coverslipped with Prolong Gold Antifade mounting medium (Fisher #P36934). For BrdU staining, sections were processed for other antibodies first then postfixed in 4% paraformaldehyde for 10 min at room temperature. Sections were then rinsed and incubated in 2N HCl (Fisher A144500) at 37°C for 30 min, followed by rinsing, blocking and primary/secondary incubation as described above. For EdU click labeling, sections were click reacted using a Click&Go EdU 488 imaging kit (Click Chemistry Tools, #1324) according to manufacturer instructions before proceeding with subsequent immunolabeling. Slides were all dried overnight at room temperature in the dark and then stored long-term at +4°C. Other materials used for tissue processing, as well as for animal treatment, are in Table 2.

Cell quantification

Similar to our previous work (Dause and Kirby, 2020), the dentate gyrus of the hippocampus was imaged in 15-μm z-stacks at 20× magnification using a Zeiss Axio Observer Z.1 with apotome digital imaging system and Axiocam 506 monochrome camera (Zeiss). EYFP+ cells were identified based on EYFP+ cytoplasm around a Hoechst+ nucleus. EYFP+ cells were considered radial glia-like neural stem cells (RGL-NSCs) if
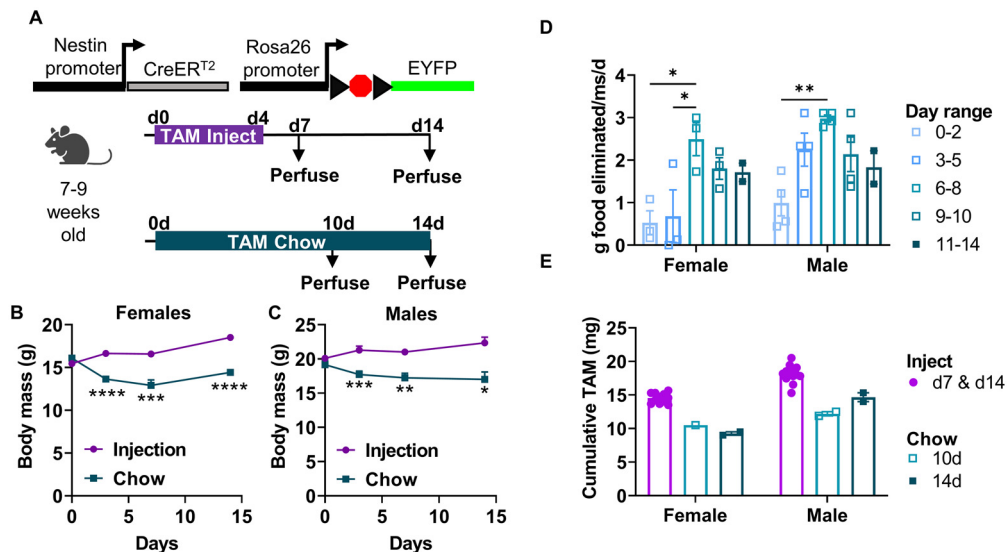
Figure 1. TAM chow causes food avoidance and results in less TAM exposure compared with TAM injection. ***A***, Experimental model and timeline. Adult Nestin-CreER^{T2}+/−;Rosa26-LoxP-STOP-LoxP-EYFP+/− mice were either injected with TAM (intraperitoneally) or voluntarily fed TAM chow. ***B***, ***C***, Body mass (in grams) of female (day: $F_{(1.637,24.56)}$ = 8.314, p = 0.0029; TAM: $F_{(1,20)}$ = 45.35, p < 0.0001; day × TAM interaction: $F_{(3,45)}$ = 23.42, p < 0.0001; ***B***) and male (day: $F_{(0.5896,9.630)}$ = 1.338, p = 0.2412; TAM: $F_{(1,23)}$ = 21.96, p = 0.0001; day × TAM interaction: $F_{(3,49)}$ = 10.40, p < 0.0001; ***C***) mice during and after TAM treatment. Mean ± SEM of n = 4–11 mice/time point. ***D***, TAM chow consumption estimation (g of food not recovered to weigh) per mouse (ms) per day, averaged within cage (sex: $F_{(1,22)}$ = 6.139, p = 0.0214; day: $F_{(4,22)}$ = 8.310, p = 0.0003; interaction: $F_{(4,22)}$ = 1.159, p = 0.3558). Mean ± SEM of n = 2–4 cages shown. ***E***, Estimated cumulative TAM exposure (milligram (mg) of TAM) in injected and chow-fed mice (sex: $F_{(1,25)}$ = 39.49, p < 0.0001; TAM: $F_{(2,25)}$ = 51.35, p < 0.0001; interaction: $F_{(2,25)}$ = 2.626, p = 0.0922). Mean ± SEM shown from n = 11–13 mice (injection) or n = 1–2 cages (chow). *p < 0.05, **p < 0.01, ***p < 0.001, ****p < 0.0001, as determined by Sidak's multiple comparisons test following a mixed-effects analysis (***B***, ***C***) or two-way ANOVA (***D***, ***E***).

they had a SOX2+ nucleus in the subgranular zone and colocalized with GFAP in the cytoplasm with an apical morphology. They were considered intermediate progenitor cells (IPCs) if they had a SOX2+ nucleus in the subgranular zone but did not have a GFAP+ cytoplasm. They were considered astrocytes if they had a SOX2+ nucleus and colocalized with GFAP in the cytoplasm with a stellate morphology. They were considered immature neurons/neuroblasts if they had a Hoechst+ nucleus in the sungranular zone and a cytoplasm that co-localized with DCX. BrdU+ cells were counted in the subgranular zone and granule cell layer throughout the dentate gyrus. Colabeling with DCX and NeuN was assessed in each BrdU+ cell in the z-stacks as surrounding DCX+ cytoplasm and/or nuclear NeuN overlap with BrdU. All cell counts were divided by dentate gyrus area sampled to yield a density of cells.

Software

Statistical analyses were performed in GraphPad Prism (version 9.3.1). Graphical abstract was made using BioRender software.

Results

TAM chow results in weight loss and less total TAM exposure compared with TAM injection

To compare TAM-induced LoxP recombination in NSPCs between injection and chow-fed methods, we crossed NestinCreER^{T2} mice (Lagace et al., 2007) with Rosa26-LoxP-STOP-LoxP-EYFP mice (Srinivas et al., 2001).

At seven to nine weeks of age, NestinCreER^{T2}+/−;Rosa26-LoxP-STOP-LoxP-EYFP+/− male and female mice were assigned randomly to either injection or chow groups. Injected mice received a standard 5-d injection regimen and were perfused on days 7 or 14 after the start of injections (Fig. 1A). TAM chow-fed mice were given free access to TAM chow for 10 or 14 d before perfusion (Fig. 1A). Both male and female TAM chow-fed mice showed lower body mass compared with TAM-injected mice (Fig. 1B,C). TAM chow-fed mice consumed very little of the chow for the first ~5 d (Fig. 1D), a time period which coincided with the greatest divergence in weight in these mice compared with TAM injected mice. Mice appeared active and well-groomed throughout the experiment. By days 6–8, male and female mice significantly increased their apparent chow consumption, coinciding with stabilization of their body weights. Cumulative TAM exposure was 1.23-fold to 1.57-fold higher in injected mice than chow-fed mice (Fig. 1E). It should be noted that some chow was crumbled on the cage floor and could not be weighed. These estimates for chow consumption are most likely overestimates. Nonetheless, these data suggest that mice find TAM chow aversive, resulting in less TAM exposure over 14 d than from 5 d of standard injections.

TAM chow results in lower recombination efficiency then TAM injections

We next compared EYFP+ cell density in the subgranular zone of the DG to determine the relative efficacy of TAM-induced Rosa26-LoxP-STOP-LoxP-EYFP recombination in

these mice. As expected based on previous studies with this line of NestinCreER[T2] mice (Lagace et al., 2007; Sun et al., 2014; Dause and Kirby, 2020), EYFP expression filled cell bodies and was strongly localized to the subgranular zone in both TAM-injected and TAM chow-fed mice (Fig. 2A). 10- and 14-d TAM chow-fed mice had 2.54-fold and 3.31-fold fewer EYFP+ cells compared with injected mice perfused 14 d after the start of injections (Fig. 2A,B; Extended Data Fig. 2-1). We next quantified the efficiency of EYFP expression specifically in GFAP+/SOX2+ RGL-NSCs and GFAP-/SOX2+ IPCs (Fig. 2C). TAM-injected mice showed EYFP expression in slightly less than half of RGL-NSCs ($47.55 \pm 6.34\%$ and $47.18 \pm 4.63\%$ at 7 and 14 d after injection start) while TAM chow-fed mice showed EYFP expression in less than a quarter of RGL-NSCs ($23.61 \pm 6.72\%$ and $13.80 \pm 2.53\%$ at 10 and 14 d of chow; Fig. 2D). Among IPCs, TAM-injected mice showed EYFP expression in $39.86 \pm 10.00\%$ and $55.91 \pm 7.65\%$ of IPCs at 7 and 14 d after injection start. TAM chow-fed mice again showed significantly less EYFP expression among IPCs ($29.89 \pm 12.72\%$ and $24.55 \pm 5.15\%$ at 10 and 14 d of chow; Fig. 2D). Separate analysis of males and females yielded similar results in each sex (Fig. 3A,B). Together, these findings suggest lower, but detectable, LoxP-recombination following 10–14 d of TAM chow feeding compared with a standard 5-d injection regimen.

TAM chow and TAM injections show similar recombination specificity

We next quantified the cell phenotype of EYFP+ cells in the DG. At day 7 after TAM injection start, $30.11 \pm 2.49\%$ of DG EYFP+ cells were phenotypic RGL-NSCs (Fig. 2E). Mice fed TAM chow for 10 d showed a similar fraction of EYFP+ cells that were phenotypic RGL-NSCs ($28.48 \pm 2.48\%$). By 14 d after TAM injection start, the percent of EYFP+ cells that were RGL-NSCs dropped significantly compared with 7 d to $17.95 \pm 1.61\%$. This decrease in proportion of EYFP+ cells that are RGL-NSCs is consistent with differentiation of the recombined, EYFP+ population over time. In the 14-d chow group, $19.28 \pm 2.47\%$ of EYFP+ cells were phenotypic RGL-NSCs, a fraction that was slightly but significantly lower than the 7-d injection group. The percent of EYFP+ cells showing IPC phenotype were similar at 7 and 14 d after injection start ($48.99 \pm 2.73\%$ and $43.44 \pm 2.73\%$; Fig. 2F). However, TAM chow-fed mice showed slightly, although significantly, higher percentages of EYFP+ cells that were phenotypic IPCs than TAM-injected mice (10 d: $54.54 \pm 3.82\%$; 14 d: $59.17 \pm 1.91\%$). As expected, very few EYFP+ cells showed an astrocytic phenotype in all groups (d7 inject: $4.00 \pm 1.45\%$; d14 inject: $0.83 \pm 0.36\%$; 10 d chow: $4.40 \pm 2.76\%$; 14 d chow: $0.61 \pm 1.38\%$; Fig. 2G). We also used co-labeling of doublecortin (DCX) with EYFP to quantify the portion of EYFP+ cells that were phenotypic neuroblasts/immature neurons. DCX co-labeling increased significantly from 7 to 14 d after TAM injection start ($28.00 \pm 2.61\%$ to $54.91 \pm 2.90\%$ of EYFP+ cells co-labeled for DCX), again consistent with the maturation of the recombined, EYFP+ cell

population over time. Both TAM chow-fed groups showed similar percentages of EYFP+ cells co-labeling for DCX as the 7-d injection group (10 d: $24.44 \pm 1.05\%$; 14 d: $26.07 \pm 2.29\%$). Separate analysis of males and females yielded similar results in each sex (Fig. 3C–F).

To assess ectopic recombination in non-neurogenic regions of the hippocampus, we quantified EYFP+ cells in CA1 and CA3. In all groups, EYFP+ cells were detectable in CA1 and CA3 but the rates of EYFP expression were low, with >92% of all EYFP+ cells being located in the dentate gyrus (Fig. 2J–K). Groups did not significantly differ from each other in EYFP localization to the dentate gyrus and separate analysis of males and females yielded similar results in each sex (Fig. 3G). All together, these data suggest that both TAM injection and TAM chow drive recombination predominantly in NSPCs with no notable differences in their specificity. They also suggest that 10–14 d of chow exposure leads to a recombined population that is most phenotypically similar to that found 7 d after TAM injection start.

TAM injection leads to a long-term suppression of cell proliferation

We next asked whether TAM exposure itself disrupts physiological adult hippocampal neurogenesis. Adult wild-type C57BL6/J mice were injected with TAM or matched dose (ml/kg) of vehicle (oil) for 5 d (Fig. 4A). Mice received daily injections of BrdU to label dividing cells coincident with the last 3 d of TAM. Mice were perfused 27 d after the first TAM injection (21 d after the last TAM/BrdU injections), 2 h after a single injection of EdU to label acutely proliferating cells. Body weights of female and male mice were not altered by 5 d TAM injection compared with vehicle injection (female: 17.38 ± 0.36 g veh vs 17.80 ± 0.38 g TAM; male: 21.93 ± 0.72 g veh vs 22.38 ± 0.46 g TAM; Fig. 4B,C). However, after a 21-d recovery from TAM/vehicle injections, TAM-injected females weighed 1.16-fold more than vehicle-injected females (17.88 ± 0.41 g veh vs 20.68 ± 0.13 g TAM; Fig. 4B). TAM and vehicle-injected body weights did not significantly differ among male mice after a 21-d recovery (23.40 ± 0.81 g veh vs 24.25 ± 0.45 g TAM; Fig. 4C).

The total density of surviving BrdU+ cells did not differ between TAM and vehicle-injected mice ($2.48 \pm 0.14 \times 10^{-4}$ vs $2.22 \pm 0.10 \times 10^{-4}$ BrdU+ cells/μm^2, respectively; Fig. 4D; Extended Data Fig. 4-1). The total density of BrdU+ cells expressing neuronal phenotypic markers DCX and/or NeuN also did not differ between TAM and vehicle-injected mice (Fig. 4E,G). Almost half of BrdU+ cells in both groups co-expressed both DCX and NeuN ($49.36 \pm 1.84\%$ veh and $46.24 \pm 1.75\%$ TAM) while slightly less than a fifth of BrdU+ cells in both groups were single positive for the mature neuronal marker NeuN ($15.82 \pm 1.47\%$ veh and $19.78 \pm 1.43\%$ TAM; Fig. 4F,G). A small proportion of BrdU+ cells were single positive for DCX ($4.12 \pm 0.91\%$ veh and $2.43 \pm 0.55\%$ TAM). Altogether, ~70% of BrdU cells showed a neuronal phenotype via DCX and/or NeuN co-labeling ($69.38 \pm 2.16\%$ veh and $68.45 \pm 1.71\%$ TAM). Similar results were found when males and females were analyzed
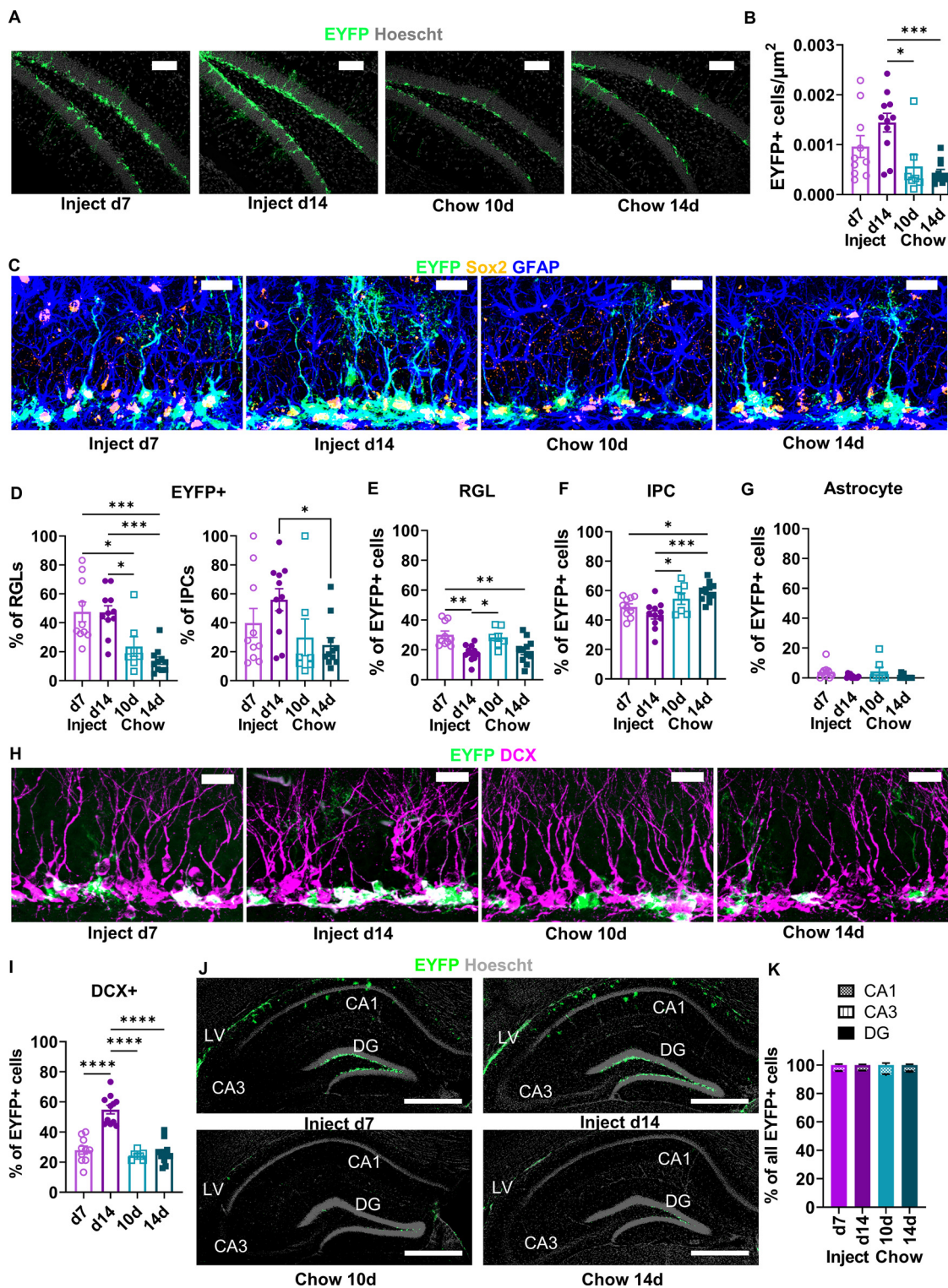
Figure 2. Recombination efficiency is higher following TAM injection than TAM diet. ***A***, Representative images of EYFP+ labeling in the DG. Scale bar: 100 μm. ***B***, Density of EYFP+ cells (cells/μm²) in the DG (ordinary one-way ANOVA, $F_{(3,35)}$ = 6.885, p = 0.0009). Mean ± SEM of n = 7–11 mice. ***C***, Representative images of EYFP, SOX2, and GFAP labeling in the dentate gyrus. Scale bar: 20 μm. ***D***, The percent of phenotypic GFAP+/SOX2+ RGL-NSCs and GFAP-/SOX2+ IPCs that were EYFP+ (RGLs: ordinary one-way ANOVA, $F_{(3,35)}$ = 11.43, p < 0.0001; IPCs: ordinary one-way ANOVA, $F_{(3,35)}$ = 2.788, p = 0.0550). Mean ± SEM of n = 7–11 mice. ***E***, The percent of EYFP+ cells that showed RGL-NSC phenotype (ordinary one-way ANOVA, $F_{(3,35)}$ = 7.531, p = 0.0005). Mean ± SEM of n = 7–11 mice. ***F***, The percent of EYFP+ cells that showed IPC phenotype (ordinary one-way ANOVA, $F_{(3,35)}$ = 7.799, p = 0.0004). Mean ± SEM of n = 7–11 mice. ***G***, The percent of EYFP+ cells that showed GFAP+ stellar astrocyte phenotype (ordinary one-way ANOVA, $F_{(3,35)}$ = 2.465, p = 0.0784). Mean ± SEM of n = 7–11 mice. ***H***, Representative images of EYFP and DCX labeling in the

continued

dentate gyrus. Scale bar: 20 µm. **I**, The percent of EYFP+ cells that were DCX+ (ordinary one-way ANOVA, $F_{(3,35)}$ = 34.97, $p < 0.0001$). Mean ± SEM of $n = 7$–11 mice. **J**, Representative images of EYFP labeling throughout the hippocampus. DG = dentate gyrus. Scale bar: 500 µm. **K**, Percent of hippocampal EYFP+ cells found in the CA1, CA3, and dentate gyrus (two-way repeated measures ANOVA; TAM × area: $F_{(6,70)}$ = 3.338, $p = 0.0060$; TAM: $F_{(3,35)}$ = 1.051, $p = 0.3822$; area: $F_{(1.186,41.50)}$ = 20 157, $p < 0.0001$; subject: $F_{(35,70)}$ = 6.492e-007, $p > 0.9999$). Mean ± SEM of $n = 7$–11 mice. *$p < 0.05$, **$p < 0.01$, ***$p < 0.001$, ****$p < 0.0001$, as determined by Tukey's multiple comparisons test.
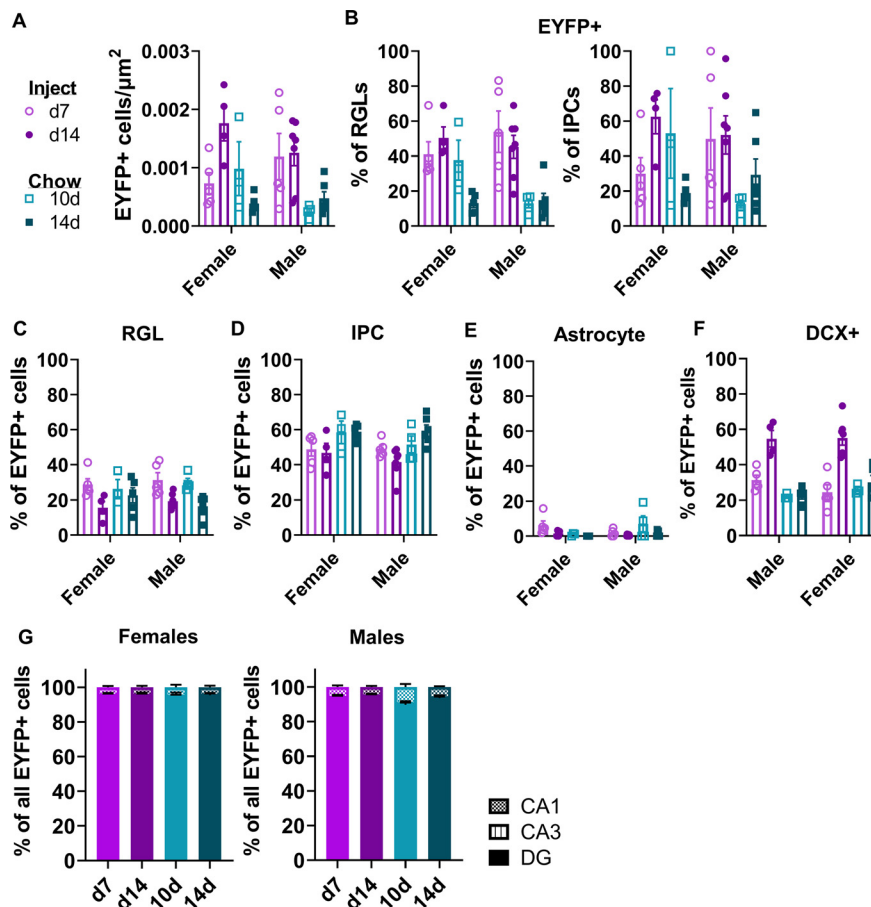
Figure 3. Recombination efficiency and labeled cell types do not depend on sex. **A**, Density of EYFP+ cells (cell/µm²) in the dentate gyrus by sex (two-way ANOVA; interaction: $F_{(3,31)}$ = 2.335, $p = 0.0931$; sex: $F_{(1,31)}$ = 0.9785, $p = 0.3302$; TAM: $F_{(3,31)}$ = 8.017, $p = 0.0004$). Mean ± SEM of $n = 3$–7 mice. **B**, The percent of phenotypic GFAP+/SOX2+ RGL-NSCs (two-way ANOVA; interaction: $F_{(3,31)}$ = 2.003, $p = 0.1341$; sex: $F_{(1,31)}$ = 0.5780, $p = 0.4528$; TAM: $F_{(3,31)}$ = 11.87, $p < 0.0001$) and GFAP-/SOX2+ IPCs (two-way ANOVA; interaction: $F_{(3,31)}$ = 2.152, $p = 0.1138$; sex: $F_{(1,31)}$ = 0.3609, $p = 0.5524$; TAM: $F_{(3,31)}$ = 3.040, $p = 0.0436$) that were EYFP+, with sex on the horizontal axis. Mean ± SEM of $n = 3$–7 mice. **C**, The percent of EYFP+ cells that showed RGL-NSC phenotype, analyzed separately by sex (two-way ANOVA; interaction: $F_{(3,31)}$ = 1.147, $p = 0.3457$; sex: $F_{(1,31)}$ = 0.1478, $p = 0.7032$; TAM: $F_{(3,31)}$ = 7.335, $p = 0.0007$). Mean ± SEM of $n = 3$–7 mice. **D**, The percent of EYFP+ cells that showed IPC phenotype, analyzed separately by sex (two-way ANOVA; interaction: $F_{(3,31)}$ = 0.4952, $p = 0.6883$; sex: $F_{(1,31)}$ = 1.078, $p = 0.3072$; TAM: $F_{(3,31)}$ = 6.650, $p = 0.0013$). Mean ± SEM of $n = 3$–7 mice. **E**, The percent of EYFP+ cells that showed GFAP+ stellar astrocyte phenotype, analyzed separately by sex (two-way ANOVA; interaction: $F_{(3,31)}$ = 2.982, $p = 0.0464$; sex: $F_{(1,31)}$ = 0.1198, $p = 0.7316$; TAM: $F_{(3,31)}$ = 2.411, $p = 0.0857$). Mean ± SEM of $n = 3$–7 mice. **F**, The percent of EYFP+ cells that showed DCX+ immature neuron phenotype, analyzed separately by sex (two-way ANOVA; interaction: $F_{(3,31)}$ = 1.580, $p = 0.2141$; sex: $F_{(1,31)}$ = 0.2172, $p = 0.6444$; TAM: $F_{(3,31)}$ = 33.62, $p < 0.0001$). Mean ± SEM of $n = 3$–7 mice. **G**, Percent of hippocampal EYFP+ cells found in the CA1, CA3, and dentate gyrus (DG) in male (two-way repeated measures ANOVA; group × region: $F_{(6,36)}$ = 6.259, $p = 0.0001$; group: $F_{(3,18)}$ = 1.636, $p = 0.2162$; region: $F_{(1.303,23.46)}$ = 14,034, $p < 0.0001$; subject: $F_{(18,36)}$ = 3.413e-007, $p > 0.9999$) and female (two-way repeated measures ANOVA; group × region: $F_{(6,26)}$ = 0.2057, $p = 0.9719$; group: $F_{(3,13)}$ = 1.090, $p = 0.3880$; region: $F_{(1.193,15.51)}$ = 12,616, $p < 0.0001$; subject: $F_{(13,26)}$ = 1.595e-006, $p > 0.9999$) mice at d7 and d14 dpi and 10 and 14 d after TAM chow initiation. Mean ± SEM of $n = 3$–5 female mice and 4–7 male mice. *$p < 0.05$, **$p < 0.01$, ***$p < 0.001$, ****$p < 0.0001$, as determined by Sidak's multiple comparisons test (**A–F**) or Tukey's multiple comparisons test (**G**).
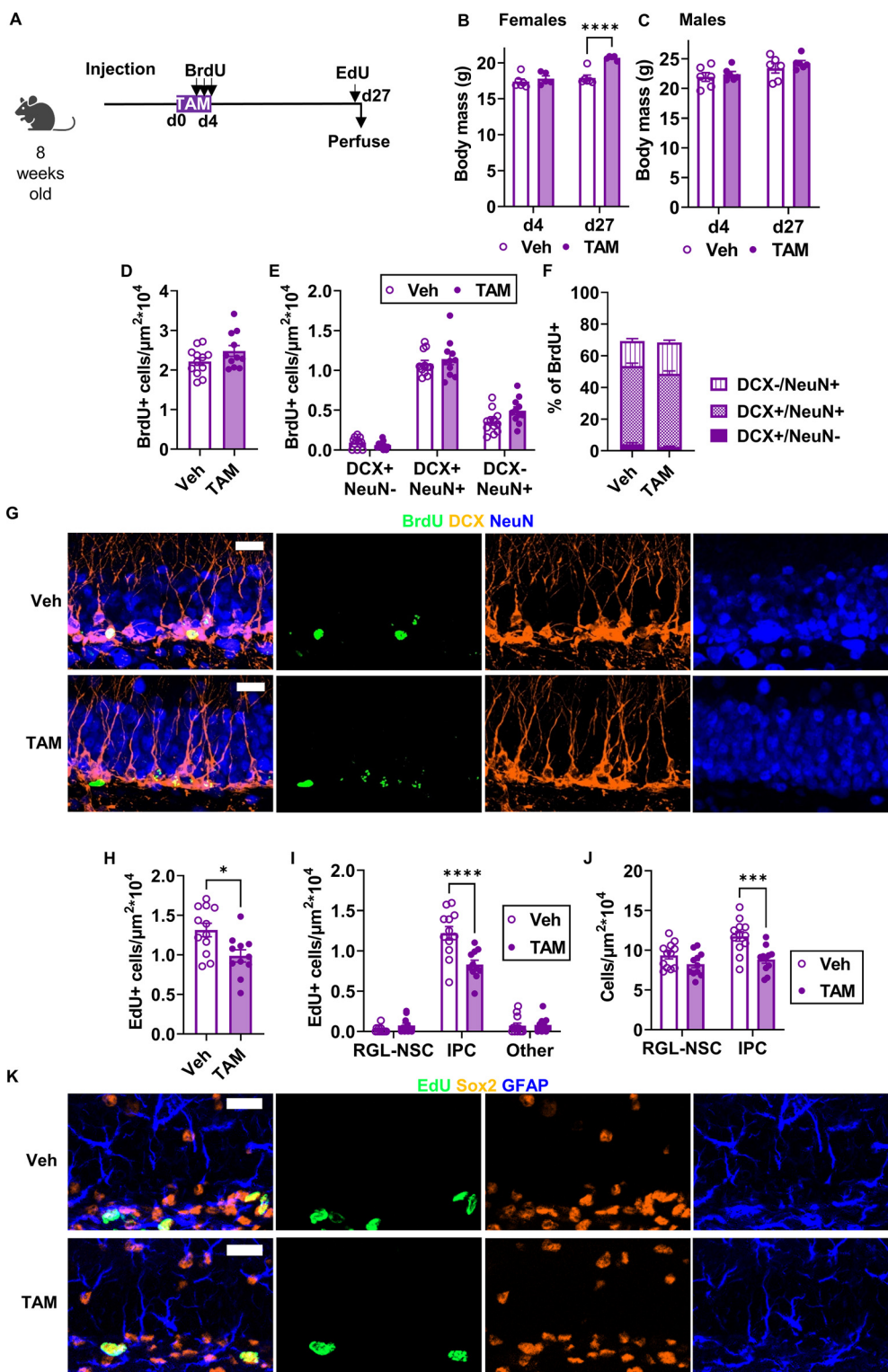
Figure 4. TAM injection suppresses progenitor cell proliferation three weeks after TAM. **A**, Experimental model and timeline. Adult wild-type mice were injected with TAM daily for 5 d then perfused three weeks later. Mice received three daily BrdU injections on the last 3 d of TAM and one EdU injection 2 h before perfusion. **B**, **C**, Average body mass of females (two-way repeated measures ANOVA; day $\times$ TAM: $F_{(1,9)} = 11.17$, $p = 0.0086$; day: $F_{(1,9)} = 22.53$, $p = 0.0010$; TAM: $F_{(1,9)} = 21.55$, $p = 0.0012$; subject: $F_{(9,9)} = 0.9448$, $p = 0.5330$) and males (two-way repeated measures ANOVA; day $\times$ TAM: $F_{(1,10)} = 0.3575$, $p = 0.5632$; day: $F_{(1,10)} = 24.83$, $p = 0.0006$; TAM: $F_{(1,10)} = 0.6152$, $p = 0.4510$; subject: $F_{(10,10)} = 6.138$, $p = 0.0042$) at the end of TAM treatment (d4) and three weeks later (d27). Mean $\pm$ SEM of $n = 5$–6 female and 6 male mice. **D**, Density of BrdU+ cells (cells/$\mu m^2 \times 10^4$) in the dentate gyrus (unpaired t test, $t_{(21)} = 1.613$, $p = 0.1217$). Mean $\pm$ SEM of $n = 11$–12 mice. **E**, Density of dentate gyrus BrdU+ cells co-labeled with DCX and/or

continued

NeuN (per $\mu m^2 \times 10^4$; two-way repeated measures ANOVA; cell type $\times$ TAM: $F_{(2,42)} = 2.461$, $p = 0.0976$; cell type: $F_{(2,42)} = 371.0$, $p < 0.0001$; TAM: $F_{(1,21)} = 1.843$, $p = 0.1890$; subject: $F_{(21,42)} = 1.698$, $p = 0.0714$). Mean $\pm$ SEM of $n = 11$–12 mice. **F**, Percent of BrdU+ dentate gyrus cells co-labeled for DCX and/or NeuN (two-way repeated measures ANOVA; cell type $\times$ TAM: $F_{(2,42)} = 3.027$, $p = 0.0591$; TAM: $F_{(1,21)} = 0.1108$, $p = 0.7425$; cell type: $F_{(1.606,33.73)} = 440.6$, $p < 0.0001$; subject: $F_{(21,42)} = 0.5522$, $p = 0.9275$). Mean $\pm$ SEM of $n = 11$–12 mice. **G**, Representative images of BrdU, DCX, and NeuN labeling. Scale bar: 20 μm. **H**, Density of EdU+ cells (cells/$\mu m^2 \times 10^4$) in the dentate gyrus (unpaired t test, $t_{(21)} = 2.814$, $p = 0.0104$). Mean $\pm$ SEM of $n = 11$–12 mice. **I**, Density (cells/$\mu m^2 \times 10^4$) of EdU+ phenotypic RGL-NSCs, IPCs, and other cells in the dentate gyrus (two-way ANOVA; interaction: $F_{(2,63)} = 13.82$, $p < 0.0001$; cell type: $F_{(2,63)} = 287.1$, $p < 0.0001$; TAM: $F_{(1,63)} = 8.275$, $p = 0.0055$). Mean $\pm$ SEM of $n = 11$–12 mice. **J**, Density (cells/$\mu m^2 \times 10^4$) of RGL-NSCs and IPCs in the dentate gyrus (two-way repeated measures ANOVA; cell type $\times$ TAM: $F_{(1,21)} = 3.203$, $p = 0.0879$; cell type: $F_{(1,21)} = 8.683$, $p = 0.0077$; TAM: $F_{(1,21)} = 15.23$, $p = 0.0008$; subject: $F_{(21,21)} = 1.029$, $p = 0.4741$). Mean $\pm$ SEM of $n = 11$–12 mice. **K**, Representative images of EdU, SOX2, and GFAP labeling. Scale bar: 20 μm. *$p < 0.05$, **$p < 0.01$, ***$p < 0.001$, ****$p < 0.0001$, as determined by Sidak's multiple comparisons test.

separately (Fig. 5A–C). Combined, these results suggest that TAM injection during BrdU-labeling does not alter the density of new-born neurons three weeks later.

We also quantified cell proliferation of RGL-NSCs and IPCs three weeks after TAM using EdU to label proliferating cells. TAM injection led to a 1.32-fold suppression of total EdU+ cell density in the dentate gyrus compared with vehicle-injected mice ($1.31 \pm 0.09 \times 10^{-4}$ cells/μm^2 veh vs $0.99 \pm 0.08 \times 10^{-4}$ cells/μm^2 TAM; Fig. 4H, K). Classification of EdU+ cells as RGL-NSCs, IPCs or neither revealed that this reduction in EdU labeling was driven primarily by loss of EdU+ IPCs (Fig. 4I,K). Quantification of total RGL-NSCs and IPCs similarly showed a significant loss of total IPC density in TAM-treated mice, with a more moderate, nonsignificant decrease in RGL-NSC density (Fig. 4J,K). Similar results were found when males and females were analyzed separately (Fig. 5D–F). These findings suggest that TAM injection causes a long-term suppression of IPC proliferation that is evident three weeks after TAM has ended.

TAM chow enhances adult neurogenesis acutely but does not suppress cell proliferation long term

To determine whether TAM chow alters adult neurogenesis, we fed adult wild-type C57BL6/J mice TAM or vehicle-matched chow for 14 d, the last three of which were coupled with once per day BrdU injections to label dividing cells (Fig. 6A). Mice were perfused 35 d after the beginning of chow treatment (21 d after the last TAM/BrdU injections), 2 h after a single EdU injection to label acutely proliferating cells. Monitoring of food consumption confirmed that during the first ~3d of chow exposure, mice consumed significantly less TAM chow than vehicle chow (2.88 ± 0.10 g veh chow/ms/d vs 1.15 ± 0.15 g TAM chow/ms/d), but consumption returned closer to vehicle chow levels shortly thereafter (Figs. 6B, 7A). Total average TAM consumption per mouse was 14.22 ± 0.95 mg, similar to that seen in Figure 1E (Figs. 6B, 7B). As expected from the TAM chow avoidance, mice that received TAM chow weighed less than vehicle chow-fed mice at the end of chow exposure, although this pattern only reached significance in the male mice (female: 16.65 ± 0.26 g veh chow vs 15.52 ± 0.31 g TAM chow; male: 22.37 ± 0.41 g veh chow vs 18.50 ± 0.45 g TAM chow; Fig. 6C,D). In females, this pattern reversed after a 21-d recovery and by

d35, TAM chow-fed mice weighed significantly more than vehicle chow-fed female mice (18.13 ± 0.25 g veh chow vs 20.00 ± 0.78 g TAM chow; Fig. 6C). TAM and vehicle-fed male mice, in contrast, no longer differed in body weight after three weeks of recovery (24.07 ± 0.32 g veh chow vs 24.18 ± 0.88 g TAM mice; Fig. 6D).

The total density of surviving BrdU+ cells did not significantly differ between TAM and vehicle chow-fed mice ($2.25 \pm 0.20 \times 10^{-4}$ cells/μm^2 vs $1.83 \pm 0.16 \times 10^{-4}$ cells/μm^2, respectively; Fig. 6E; Extended Data Fig. 6-1). In contrast, the density of BrdU+ cells co-expressing both DCX and NeuN was significantly higher in TAM chow-fed mice than vehicle-fed mice ($0.64 \pm 0.06 \times 10^{-4}$ cells/μm^2 veh chow vs $1.10 \pm 0.14 \times 10^{-4}$ cells/μm^2 TAM chow; Fig. 6F,H). The percent of BrdU+ cells co-expressing both DCX and NeuN was similarly higher in the TAM chow-fed mice than vehicle chow-fed mice ($35.15 \pm 2.17\%$ veh chow vs $48.09 \pm 3.42\%$ TAM chow; Fig. 6G). The percentage of BrdU+ cells single positive for DCX or NeuN was small in both groups and did not differ between groups (DCX: $8.46 \pm 1.26\%$ veh chow vs $7.915 \pm 1.63\%$ TAM chow; NeuN: $11.38 \pm 1.31\%$ veh chow vs $11.42 \pm 1.57\%$ TAM chow). Similar results were found when males and females were analyzed separately (Fig. 7C–E). These results suggest that the TAM chow exposure paradigm drives more neurogenesis primarily via enhanced neuronal differentiation of cells proliferating during TAM exposure.

We also quantified cell proliferation of RGL-NSCs and IPCs three weeks after TAM using EdU to label proliferating cells. EdU+ cell density in the DG did not significantly differ between veh and TAM chow-fed mice ($1.21 \pm 0.12 \times 10^{-4}$ cells/μm^2 veh vs $1.06 \pm 0.07 \times 10^{-4}$ cells/μm^2 TAM; Fig. 6I,L). Classification of EdU+ cells as RGL-NSCs, IPCs or neither similarly showed no difference in EdU+ density of these cell subtypes between chow groups (Fig. 6J,L). Quantification of total RGL-NSCs and IPCs also showed no difference in total RGL-NSC or IPC density (Fig. 6K,L). Similar results were found when males and females were analyzed separately (Fig. 7F–H). These findings suggest that TAM chow feeding does not strongly alter cell proliferation relative to vehicle chow three weeks after chow treatment has ended.

Discussion

In this work, we found that TAM chow treated mice showed less recombination efficiency but similar
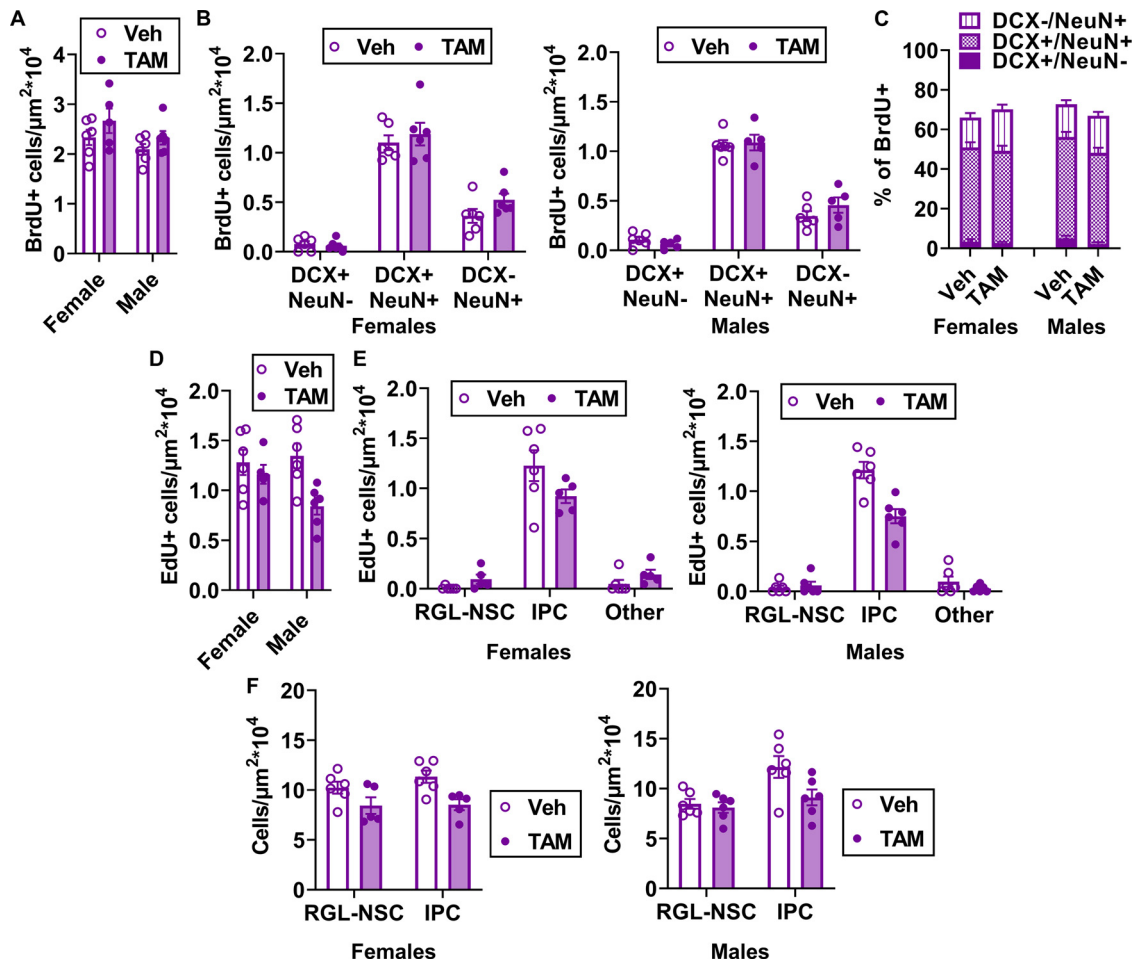
Figure 5. TAM injection effects on cell survival and proliferation do not differ by sex. **A**, Density of BrdU+ cells (cells/$\mu m^2 \times 10^4$) in the dentate gyrus (two-way ANOVA; interaction: $F_{(1,19)} = 0.09813$, $p = 0.7575$; sex: $F_{(1,19)} = 3.232$, $p = 0.0881$; TAM: $F_{(1,19)} = 3.076$, $p = 0.0956$). Mean $\pm$ SEM of $n = 5–6$ mice. **B**, Density of dentate gyrus BrdU+ cells (cells/$\mu m^2 \times 10^4$) co-labeled with DCX and/or NeuN (three-way repeated measures ANOVA; cell type: $F_{(1.823,34.63)} = 343.0$, $p < 0.0001$; sex: $F_{(1,19)} = 0.5866$, $p = 0.4531$; TAM: $F_{(1,19)} = 1.581$, $p = 0.2238$; cell type $\times$ sex: $F_{(2,38)} = 0.5649$, $p = 0.5731$; cell type $\times$ TAM: $F_{(2,38)} = 2.197$, $p = 0.1250$; sex $\times$ TAM: $F_{(1,19)} = 0.2991$, $p = 0.5908$; cell type $\times$ sex $\times$ TAM: $F_{(2,38)} = 0.02294$, $p = 0.9773$). Mean $\pm$ SEM of $n = 6$ female mice and 5–6 male mice. **C**, Percent of BrdU+ dentate gyrus cells labeled for DCX and/or NeuN (three-way repeated measures ANOVA; cell type: $F_{(1.608,30.55)} = 401.7$, $p < 0.0001$; sex: $F_{(1,19)} = 0.4138$, $p = 0.5277$; TAM: $F_{(1,19)} = 0.08557$, $p = 0.7731$; cell type $\times$ sex: $F_{(2,38)} = 0.1847$, $p = 0.8321$; cell type $\times$ TAM: $F_{(2,38)} = 2.828$, $p = 0.0716$; sex $\times$ TAM: $F_{(1,19)} = 3.418$, $p = 0.0801$; cell type $\times$ sex $\times$ TAM: $F_{(2,38)} = 0.04,942$), $p = 0.9518$. Mean $\pm$ SEM of $n = 5–6$ mice. **D**, Density of EdU+ cells (cells/$\mu m^2 \times 10^4$) in the dentate gyrus (two-way ANOVA; interaction: $F_{(1,19)} = 2.991$, $p = 0.0999$; sex: $F_{(1,19)} = 1.313$, $p = 0.2660$; TAM: $F_{(1,19)} = 7.928$, $p = 0.0110$). Mean $\pm$ SEM of $n = 5–6$ mice. **E**, Density (cells/$\mu m^2 \times 10^4$) of dentate gyrus EdU+ phenotypic RGL-NSCs, IPCs, and other cells (three-way repeated measures ANOVA; cell type: $F_{(2,38)} = 274.4$, $p < 0.0001$; sex: $F_{(1,19)} = 1.313$, $p = 0.2660$; TAM: $F_{(1,19)} = 7.928$, $p = 0.0110$; cell type $\times$ sex: $F_{(2,38)} = 0.4635$, $p = 0.6326$; cell type $\times$ TAM: $F_{(2,38)} = 12.86$, $p < 0.0001$; sex $\times$ TAM: $F_{(1,19)} = 2.991$, $p = 0.0999$; cell type $\times$ sex $\times$ TAM: $F_{(2,38)} = 0.1659$, $p = 0.8477$). Mean $\pm$ SEM of $n = 5–6$ female mice and 6 male mice. **F**, Density (cells/$\mu m^2 \times 10^4$) of RGL-NSCs and IPCs in the dentate gyrus, by sex (three-way repeated measures ANOVA; cell type: $F_{(1,19)} = 9.308$, $p = 0.0066$; sex: $F_{(1,19)} = 0.1083$, $p = 0.7457$; TAM: $F_{(1,19)} = 14.12$, $p = 0.0013$; cell type $\times$ sex: $F_{(1,19)} = 3.346$, $p = 0.0831$; cell type $\times$ TAM: $F_{(1,19)} = 3.699$, $p = 0.0696$; sex $\times$ TAM: $F_{(1,19)} = 0.3142$, $p = 0.5817$; cell type $\times$ sex $\times$ TAM: $F_{(1,19)} = 0.7541$, $p = 0.3960$). Mean $\pm$ SEM of $n = 5–6$ female mice and 6 male mice. *$p < 0.05$, **$p < 0.01$, ***$p < 0.001$, ****$p < 0.0001$, as determined by Sidak's multiple comparisons test.

recombination specificity as TAM-injected mice in a commonly used NestinCreER^{T2} model that targets recombination in adult NSPCs. Both administration protocols also had inherent, although different, effects on adult neurogenesis. The TAM injection protocol suppressed IPC proliferation three weeks after TAM, whereas the TAM chow protocol did not disrupt later IPC proliferation but did induce greater neuronal differentiation of cells born during TAM. Altogether, our results suggest that both

administration routes of TAM are potentially useful but selection of controls requires attention to the inherent effects of TAM delivery.

The difference between TAM injection and TAM chow in recombination efficiency is most likely explained by total TAM exposure. Recombination efficiency in TAM-inducible transgenic systems is partly dose dependent (Hayashi and McMahon, 2002), and mice given TAM chow were exposed to overall less TAM than those given TAM injections. Mice
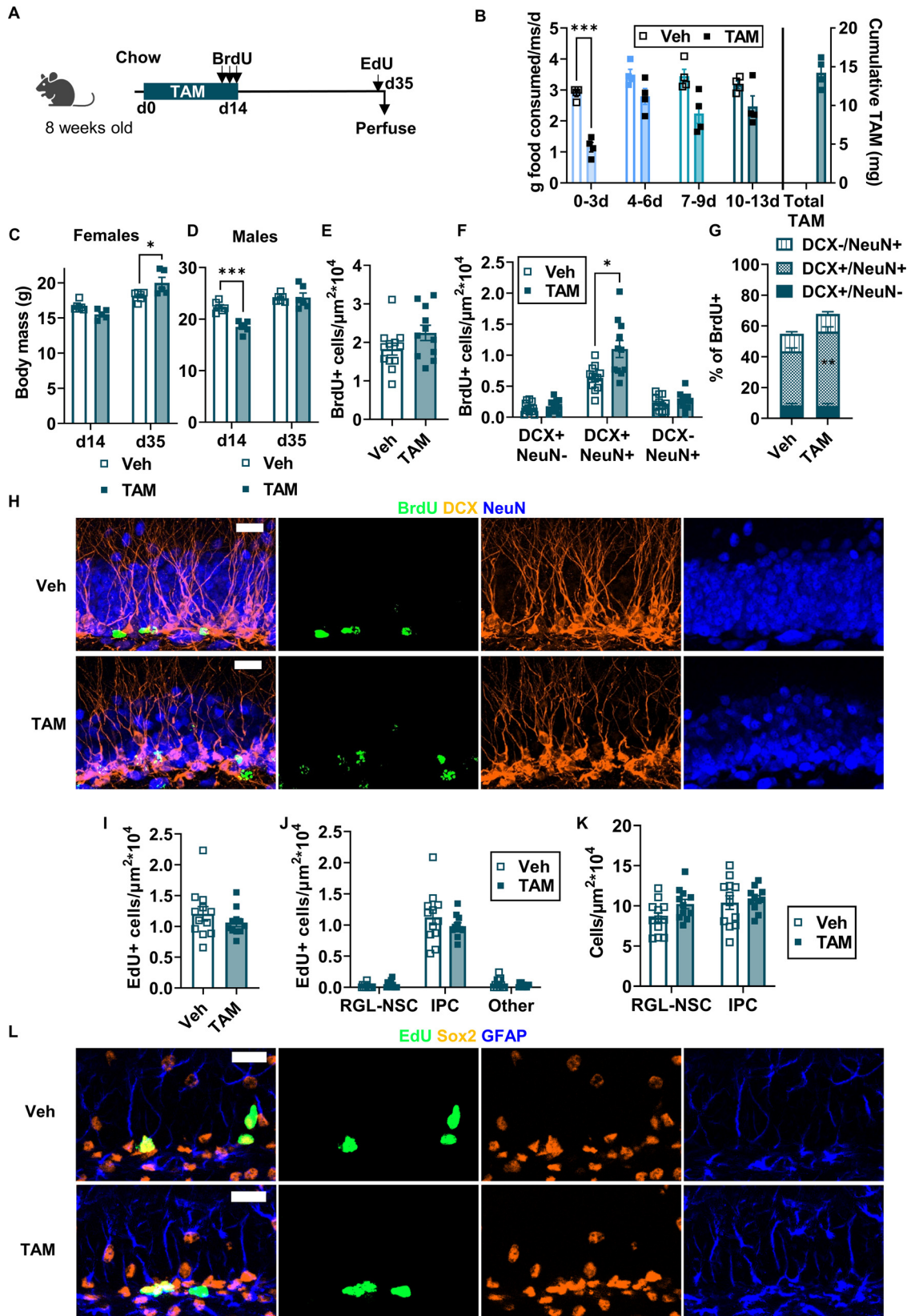
Figure 6. TAM chow alters the phenotype of surviving cells 35 d after initial exposure. **A**, Experimental model and timeline. Mice were injected with BrdU in the last 3 d of the 14-d TAM chow period. EdU was injected 35 d after initial chow exposure. **B**, Grams of food consumed per mouse (ms) per day over each 3- to 4-d period of diet exposure and TAM consumed in milligrams (mg) (two-way repeated measures ANOVA; day × TAM: $F_{(3,18)} = 2.322$, $p = 0.1095$; day: $F_{(1.564,9.384)} = 8.978$, $p = 0.0088$; TAM: $F_{(1,6)} = 45.86$, $p = 0.0005$; subject:

continued

$F_{(6,18)} = 0.9896$, $p = 0.4613$). Mean $\pm$ SEM of $n = 4$ mice. **C,** In female mice, body mass in grams 14 and 35 d after diet initiation (two-way repeated measures ANOVA; day $\times$ TAM: $F_{(1,9)} = 10.62$, $p = 0.0099$; day: $F_{(1,9)} = 42.05$, $p = 0.0001$; TAM: $F_{(1,9)} = 0.8454$, $p = 0.3818$; subject: $F_{(9,9)} = 0.7591$, $p = 0.6560$). Mean $\pm$ SEM of $n = 5$–6 mice. **D,** In male mice, body mass in grams 14 and 35 d after diet initiation (two-way repeated measures ANOVA; day $\times$ TAM: $F_{(1,10)} = 18.18$, $p = 0.0017$; day: $F_{(1,10)} = 62.45$, $p < 0.0001$; TAM: $F_{(1,10)} = 8.540$, $p = 0.0152$; subject: $F_{(10,10)} = 1.886$, $p = 0.1658$). Mean $\pm$ SEM of $n = 6$ mice. **E,** Density of BrdU+ cells (cells/$\mu m^2 \times 10^4$) in the dentate gyrus (unpaired t test, $t_{(21)} = 1.675$, $p = 0.1087$). Mean $\pm$ SEM of $n = 11$–12 mice. **F,** Density of dentate gyrus BrdU+ cells (cells/$\mu m^2 \times 10^4$) co-labeled with DCX and/or NeuN (two-way repeated measures ANOVA; cell type $\times$ TAM: $F_{(2,42)} = 8.654$, $p = 0.0007$; cell type: $F_{(1.207,25.35)} = 83.41$, $p < 0.0001$; TAM: $F_{(1,21)} = 8.675$, $p = 0.0077$; subject: $F_{(21,42)} = 1.516$, $p = 0.1239$). Mean $\pm$ SEM of $n = 11$–12 mice. **G,** Percent of BrdU+ dentate gyrus cells labeled for DCX and/or NeuN (two-way repeated measures ANOVA; TAM $\times$ cell type: $F_{(2,42)} = 6.501$, $p = 0.0035$; TAM: $F_{(1,21)} = 16.13$, $p = 0.0006$; cell type: $F_{(1.545,32.44)} = 151.5$, $p < 0.0001$; subject: $F_{(21,42)} = 0.3789$, $p = 0.9903$). Mean $\pm$ SEM of $n = 11$–12 mice. **H,** Representative images of BrdU, DCX, and NeuN labeling. Scale bar: 20 μm. **I,** Density of EdU+ cells (cells/$\mu m^2 \times 10^4$) in the dentate gyrus (unpaired t test, $t_{(21)} = 1.043$, $p = 0.3090$). Mean $\pm$ SEM of $n = 11$–12 mice. **J,** Density (cells/$\mu m^2 \times 10^4$) of dentate gyrus EdU+ phenotypic RGL-NSCs, IPCs, and other cells (two-way repeated measures ANOVA; cell type $\times$ TAM: $F_{(2,42)} = 1.157$, $p = 0.3241$; cell type: $F_{(1.066,22.38)} = 210.3$, $p < 0.0001$; TAM: $F_{(1,21)} = 1.087$, $p = 0.3090$; subject: $F_{(21,42)} = 0.9645$, $p = 0.5209$). Mean $\pm$ SEM of $n = 11$–12 mice. **K,** Density (cells/$\mu m^2 \times 10^4$) of RGL-NSCs and IPCs in the dentate gyrus (two-way repeated measures ANOVA; cell type $\times$ TAM: $F_{(1,21)} = 1.042$, $p = 0.3191$; cell type: $F_{(1,21)} = 3.794$, $p = 0.0649$; TAM: $F_{(1,21)} = 2.404$, $p = 0.1360$; subject: $F_{(21,21)} = 1.138$, $p = 0.3846$). Mean $\pm$ SEM of $n = 11$–12 mice. **L,** Representative images of EdU, SOX2, and GFAP labeling. Scale bar: 20 μm. *$p < 0.05$, **$p < 0.01$, ***$p < 0.001$, ****$p < 0.0001$, as determined by Sidak's multiple comparisons test.

showed strong aversion to the TAM chow, as evidenced by the approximately one-week delay between chow introduction and substantial daily consumption. It is not surprising then to observe substantially less recombination in chow mice than injected mice. The chow was sweetened to increase palatability and delivered on the cage floor in dishes to ease access, so future efforts to overcome this barrier to TAM ingestion may require longer TAM chow treatments. In studies targeting adult neurogenic processes, however, longer chow treatment will result in a

Table 2: Other reagents used

Item	Vendor	Product number	RRID or link
NestinCreER[T2] mice	The Jackson Laboratory	#016261	IMSR_JAX:016261
R26R-LoxP-STOP-LoxP-EYFP	The Jackson Laboratory	#007909	IMSR_JAX:007909
BrdU	Sigma	#B5002	https://www.sigmaaldrich.com/US/en/product/sigma/b5002?gclid=Cj0KCQiAjJOQBhCkARIsAEKMtO2Z8yDVbyW9L9oduQd8T7l-a8P6oFzW-2kKfd-oo4Nm87mNJH-mzwZQaAgXJEALw_wcB
EdU	Click Chemistry Tools	#1149-500	https://clickchemistrytools.com/product/5-ethynyl-2%E2%80%B2-deoxyuridine-edu/
TAM chow	Envigo	TD.130858	https://www.envigo.com/tamoxifen-custom-diets
Paraformaldehyde	Fisher	#AC169650010	https://www.fishersci.com/shop/products/paraformaldehyde-90-pure-thermo-scientific/AC169650010
Sucrose	Fisher	S5-3	https://www.fishersci.com/shop/products/sucrose-crystalline-certified-acs-fisher-chemical-3/S53#?keyword=S5-3
PBS	Fisher	#BP399-20	https://www.fishersci.com/shop/products/pbs-phosphate-buffered-saline-10x-solution-fisher-bioreagents/BP39920?searchHijack=true&searchTerm=BP399-20&searchType=RAPID&matchedCatNo=BP399-20
Normal donkey serum	Jackson ImmunoResearch	#017000121	AB_2337258
Triton X-100	Fisher	#AAA16046AE	https://www.fishersci.com/shop/products/triton-x-100-thermo-scientific/AAA16046AE?searchHijack=true&searchTerm=triton-x-100-thermo-scientific&searchType=Rapid&matchedCatNo=AAA16046AE
Hoechst 33342	Fisher	#H3570	https://www.fishersci.com/shop/products/molecular-probes-hoechst-33342-trihydrochloride-trihydrate/H3570#?keyword=H3570
SuperFrost Plus slides	Fisher	#12-550-15	https://www.fishersci.com/shop/products/fisherbrand-superfrost-plus-microscope-slides-2/1255015#?keyword=12-550-15
Prolong Gold Antifade mounting medium	Fisher	#P36934	https://www.fishersci.com/shop/products/molecular-probes-prolong-gold-antifade-mountant-5/P36934?searchHijack=true&searchTerm=P36934&searchType=RAPID&matchedCatNo=P36934
12N HCl	Fisher	A144500	https://www.fishersci.com/shop/products/hydrochloric-acid-certified-acs-plus-fisher-chemical-10/A144500#?keyword=A144500
Click&Go EdU 488 imaging kit	Click Chemistry Tools	#1324	https://clickchemistrytools.com/product/click-go-edu-488-imaging-kit/

List of other major reagents.
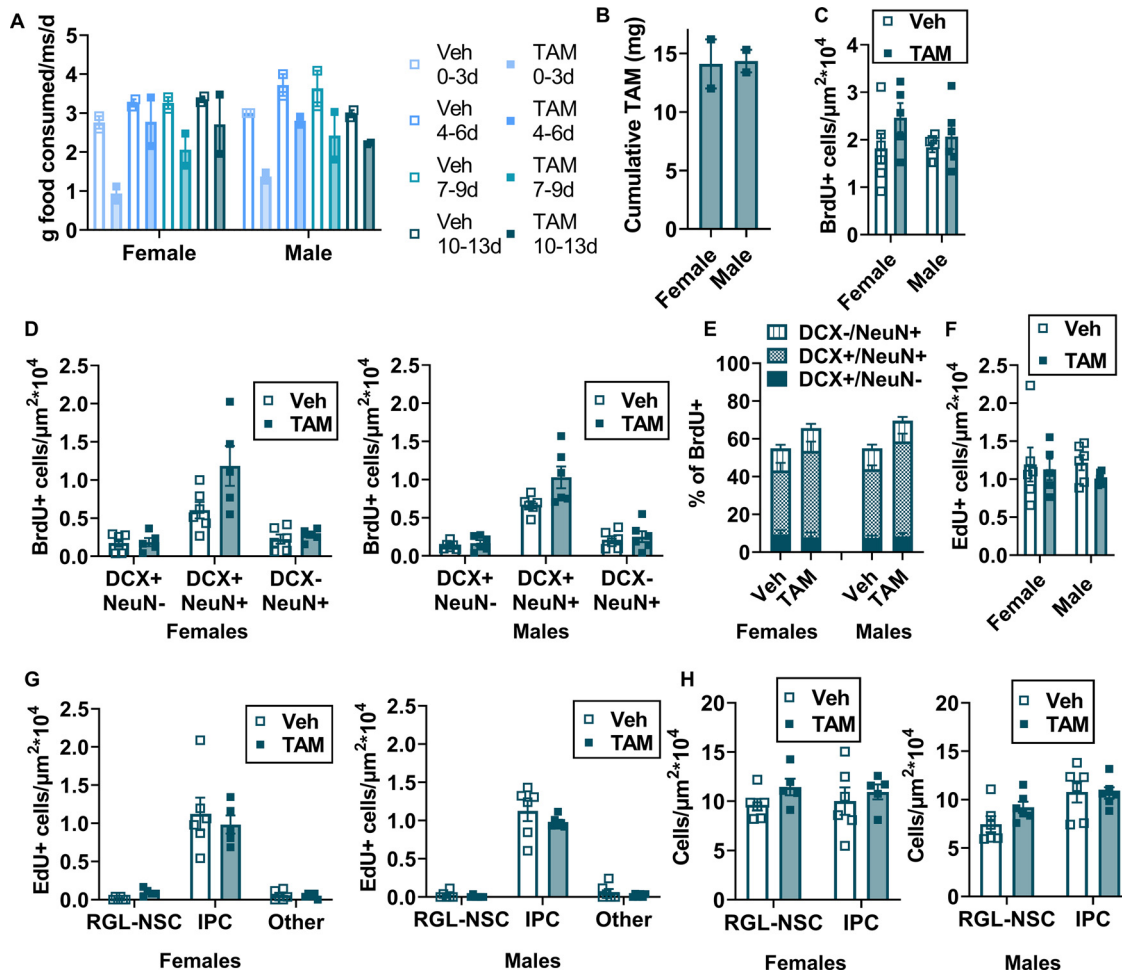
Figure 7. TAM diet effects on cell survival and proliferation do not differ by sex. ***A***, Grams of TAM and vehicle chow consumed by male ($n = 2$ cages/sex) and female ($n = 2$ cages/sex) mice per mouse (ms) per day over each 3- to 4-d period of diet exposure. ***B***, Cumulative TAM consumed in milligrams (mg) by sex ($n = 2$ cages/sex). ***C***, Density of BrdU+ cells (cells/$\mu m^2 \times 10^4$) in the dentate gyrus, by sex (two-way ANOVA; interaction: $F_{(1,19)} = 0.6818$, $p = 0.4192$; sex: $F_{(1,19)} = 0.5413$, $p = 0.4709$; TAM: $F_{(1,19)} = 2.921$, $p = 0.1037$). Mean $\pm$ SEM of $n = 5$–6 mice. ***D***, Density of dentate gyrus BrdU+ cells (cells/$\mu m^2 \times 10^4$) co-labeled with DCX and/or NeuN in females and males (three-way repeated measures ANOVA: cell type: $F_{(1.213,23.05)} = 78.09$, $p < 0.0001$; sex: $F_{(1,19)} = 0.2586$, $p = 0.6169$; TAM: $F_{(1,19)} = 8.323$, $p = 0.0095$; cell type $\times$ sex: $F_{(2,38)} = 0.02142$, $p = 0.9788$; cell type $\times$ TAM: $F_{(2,38)} = 8.256$, $p = 0.0011$; sex $\times$ TAM: $F_{(1,19)} = 0.3225$, $p = 0.5767$; cell type $\times$ sex $\times$ TAM: $F_{(2,38)} = 0.5548$, $p = 0.5787$). Mean $\pm$ SEM of $n = 5$–6 female mice and 6 male mice. ***E***, Percent of BrdU+ dentate gyrus cells labeled for DCX and/or NeuN in male and female mice (three-way repeated measures ANOVA: cell type: $F_{(1.557,29.58)} = 140.5$, $p < 0.0001$; sex: $F_{(1,19)} = 0.3592$, $p = 0.5561$; TAM: $F_{(1,19)} = 14.62$, $p = 0.0011$; cell type $\times$ sex: $F_{(2,38)} = 0.6323$, $p = 0.5369$; cell type $\times$ TAM: $F_{(2,38)} = 5.877$, $p = 0.0060$; sex $\times$ TAM: $F_{(1,19)} = 0.3233$, $p = 0.5763$; cell type $\times$ sex $\times$ TAM: $F_{(2,38)} = 0.06,331$, $p = 0.9387$). Mean $\pm$ SEM of $n = 5$–6 mice. ***F***, Density of EdU+ cells (cells/$\mu m^2 \times 10^4$) in the dentate gyrus in male and female mice (two-way ANOVA; interaction: $F_{(1,19)} = 0.2581$, $p = 0.6173$; sex: $F_{(1,19)} = 0.1190$, $p = 0.7339$; TAM: $F_{(1,19)} = 0.9220$, $p = 0.3490$). Mean $\pm$ SEM of $n = 5$–6 mice. ***G***, Density (cells/$\mu m^2 \times 10^4$) of dentate gyrus EdU+ phenotypic RGL-NSCs, IPCs, and other cells in male and female mice (three-way ANOVA: cell type: $F_{(1.058,20.10)} = 190.3$, $p < 0.0001$; sex: $F_{(1,19)} = 0.1190$, $p = 0.7339$; TAM: $F_{(1,19)} = 0.9220$, $p = 0.3490$; cell type $\times$ sex: $F_{(2,38)} = 0.05511$, $p = 0.9465$; cell type $\times$ TAM: $F_{(2,38)} = 1.094$, $p = 0.3451$; sex $\times$ TAM: $F_{(1,19)} = 0.2581$, $p = 0.6173$; cell type $\times$ sex $\times$ TAM: $F_{(2,38)} = 0.08267$, $p = 0.9208$). Mean $\pm$ SEM of $n = 5$–6 female mice and 6 male mice. ***H***, Density (cells/$\mu m^2 \times 10^4$) of RGL-NSCs and IPCs in the dentate gyrus of male and female mice (three-way ANOVA: cell type: $F_{(1,19)} = 3.943$, $p = 0.0617$; sex: $F_{(1,19)} = 2.181$, $p = 0.1561$; TAM: $F_{(1,19)} = 2.703$, $p = 0.1166$; cell type $\times$ sex: $F_{(1,19)} = 4.370$, $p = 0.0503$; cell type $\times$ TAM: $F_{(1,19)} = 1.338$, $p = 0.2618$; sex $\times$ TAM: $F_{(1,19)} = 0.1703$, $p = 0.6845$; cell type $\times$ sex $\times$ TAM: $F_{(1,19)} = 0.1708$, $p = 0.6840$). Mean $\pm$ SEM of $n = 5$–6 female mice and 6 male mice. $*p < 0.05$, $**p < 0.01$, $***p < 0.001$, $****p < 0.0001$, as determined by Sidak's multiple comparisons test.

more heterogenous population of recombined cells at different stages of differentiation. Temporal precision is often a goal of adult neurogenesis studies, and extending chow treatment times may not always fit with that goal. Another possibility would be to provide

TAM via oral gavage. However, oral gavage is notoriously stressful for animals (Brown et al., 2000) and requires expertise on the part of the experimenter to reduce that stress and avoid injury to animals (Arantes-Rodrigues et al., 2012). If high recombination

efficiency and selective targeting of cells of similar maturity are desired, our data suggest that TAM injections are still the preferable method.

Despite differences in recombination efficiency between the TAM administration routes tested here, this work also shows that two weeks of TAM chow induces genetic recombination with similar specificity to 5 d of TAM injection. Mice fed TAM chow for two weeks showed a recombined cell population of similar phenotype (primarily NSPCs) as TAM-injected mice 7 d after the start of injections. Thus, TAM-infused chow could be a workable alternative administration route when TAM injection is not feasible, when lower recombination efficiency is desired, or when long-term suppression of cell proliferation would interfere with interpretation of experimental results.

Our findings comparing TAM versus vehicle-injected mice provide several useful insights into the effects of this commonly-used agent on adult neurogenesis. First, we found that neurogenesis derived from cells born during TAM was not substantially affected by TAM injection. These results are similar to those reported in (Rotheneichner et al., 2017), which showed no difference in BrdU+ cell density or phenotype between TAM and vehicle-injected mice 10 d after TAM/BrdU using five-month-old male and female mice. In contrast, using three- to four-week-old (juvenile) male mice, Lee et al. (2020) found that the density of surviving BrdU+ cells approximately one week after TAM/BrdU was suppressed by ~2-fold in TAM-injected versus vehicle-injected mice. Combined, these findings suggest that the effect of TAM injection on production of new DG cells that survive 1+ weeks could depend on organismal age. Sex may also be a factor, but this is difficult to discern as previous work either used only males or did not show data for males and females separately. Future research is needed to address the effects of TAM on cell proliferation and survival to better understand how TAM affects neurogenesis across the lifespan and in both sexes.

Second, we show that TAM injection had prolonged effects on progenitor cell proliferation, suppressing progenitor density and proliferation by ~1.3-fold three weeks after TAM. Lee and colleagues similarly reported a ~1.8-fold TAM-induced suppression of Mki67-labeled progenitors one week after TAM in juvenile mice. Rotheneichner et al. (2017) reported no difference in PCNA+ progenitor cell number 10 d after TAM in their five-month-old mice, however. Again, this difference may reflect increased susceptibility of juvenile mice to the effects of TAM, a subtle sex difference, or a time point effect.

The mechanism by which TAM suppresses progenitor proliferation weeks after TAM treatment is unclear. One possible mechanism for suppression of cell proliferation associated with TAM treatment in general is brain estrogen receptor modulation by TAM. TAM acts on brain $ER\alpha$, $ER\beta$, and the transmembrane receptor GPR30 (Gonzalez et al., 2016). Specifically, TAM can be an estrogen agonist at GPR30 (Filardo et al., 2000; Vivacqua et al., 2006a,b) and $ER\beta$ (McDonnell and Wardell, 2010), and it can induce estrogen blockade at $ER\alpha$ (McDonnell and Wardell,

2010). Because $ER\alpha$ agonists can enhance cell proliferation in the adult hippocampus (Mazzucco et al., 2006), it therefore seems possible that TAM blockade of $ER\alpha$ could suppress proliferation. Receptor-independent effects on cell cycle genes, as proposed by Lee et al. (2020), are also a potential mechanism of TAM-induced suppression of proliferation. With either mechanism, however, it is unclear why those effects would persist long after TAM withdrawal. TAM metabolites remain in the brain for ~8 d after administration (Valny et al., 2016), making it unlikely that suppression of proliferation three weeks later is a result of active TAM presence. This long-term persistence could therefore be because initial effects of TAM are slow to arise and/or indelible (e.g., epigenetic changes), or because they reflect effects of TAM withdrawal rather than TAM itself. Future research is needed to parse out these multiple, nonexclusive hypotheses.

We also noted delayed weight gain in female mice that received TAM injection, resulting in higher average body mass of TAM treated females than vehicle treated females three weeks after injection. Because TAM was administered systemically, this delayed weight gain in female mice could be because of TAM effects on multiple central or peripheral tissues. One candidate tissue is the hypothalamus. In mice, hypothalamic $ER\alpha$-dependent gene expression changes have been linked to common TAM side effects, including decreased movement (Zhang et al., 2021), which could contribute to weight gain.

TAM chow had qualitatively different effects on neurogenesis and cell proliferation than TAM injection. In contrast to TAM injections, TAM chow increased neuronal differentiation of cells born during TAM but had no effect on density of EdU+ cells three weeks after TAM. Caloric restriction and reduced total TAM exposure in chow-fed mice (compared with TAM-injected mice) both likely contribute to this difference between paradigms. Caloric restriction is a particularly important confounding factor to consider when comparing TAM chow-fed to vehicle chow-fed animals. Although Bondolfi and colleagues found no effect of caloric restriction on hippocampal neurogenesis in male mice aged 3–11 months (Bondolfi et al., 2004), others have found that dietary restriction and intermittent fasting enhance neuronal differentiation in the adult hippocampus (Hornsby et al., 2016; Li et al., 2020). Both the caloric restriction during TAM feeding and the return to normal feeding after the end of TAM chow may therefore be affecting neurogenesis in TAM-fed mice. Regardless of the reason for differing effects of TAM by administration route, our data further underscore the need for internal TAM-treated controls in experiments using TAM chow, just as with TAM injection.

Limitations and future directions

Because mice often crumble food and spread it across the floor of the cage, we are unable to account for chow that was chewed in this manner but not consumed. Our calculations of the amount of TAM chow consumed are almost certainly overestimations. This is a limitation of using chow that others may want to consider when

knowing exact TAM amounts is critical to study design or interpretation.

Because this work examines direct TAM effects on experimental endpoints only in the context of neurogenesis research in adult animals, further testing is needed to determine the suitability of alternate TAM dosing methods for subadult animals and research on other brain processes. Also, our BrdU+ counts reflect both cell proliferation during TAM administration and post-TAM cell survival, making it difficult to disentangle TAM effects on either process independently. Thymidine analogs, such as the BrdU and EdU we used here, mark only a subset of proliferating cells, so it is possible that further or fewer differences would be observed if all proliferating cells were labeled (with a mitotic marker such as PCNA or MCM2) and assessed. It is also possible that any or all of the effects observed in this study could vary throughout the anatomy of the dentate gyrus (dorsal vs ventral, inferior vs superior blades of the subgranular zone). Our counts reflect areas sampled throughout the DG and therefore do not capture this information. In addition, although we provide the parental source of NestinCreER^{T2} in Extended Data Figure 2-1, we do not have sufficient sample size to draw conclusions about the effect of inheriting maternal versus paternal NestinCreER^{T2} on any of the outcome measures.

Better understanding of the molecular mechanism by which TAM acts on adult neurogenesis, when provided by injection or chow, is also still needed, as is further assessment of how (if at all) TAM differentially affects reporter-labeled and nonlabeled cell populations. Finally, clarity regarding the actions of TAM on brain estrogen receptors is lacking and could help guide researchers' choice of TAM dosing methods and interpretation of studies where TAM is used.

In conclusion, this work shows that voluntary TAM chow consumption may be a suitable alternative to TAM injections for inducing Cre-lox recombination in some adult neurogenesis studies. This work further identifies several effects of TAM administration protocols, whether by injection or food, on adult neurogenesis endpoints. These effects are separate from genetic recombination effects and are an important confounding variable in experimental designs that rely on comparisons to a vehicle-treated control. Thus, we suggest that research using TAM-inducible Cre lines use TAM-treated wild-type (non-recombination susceptible) littermates as controls, rather than vehicle-treated mice.

References

Arantes-Rodrigues R, Henriques A, Pinto-Leite R, Faustino-Rocha A, Pinho-Oliveira J, Teixeira-Guedes C, Seixas F, Gama A, Colaço B, Colaço A, Oliveira PA (2012) The effects of repeated oral gavage on the health of male CD-1 mice. Lab Anim (NY) 41:129–134.

Bondolfi L, Ermini F, Long JM, Ingram DK, Jucker M (2004) Impact of age and caloric restriction on neurogenesis in the dentate gyrus of C57BL/6 mice. Neurobiol Aging 25:333–340.

Brown AP, Dinger N, Levine BS (2000) Stress produced by gavage administration in the rat. Contemp Top Lab Anim Sci 39:17–21.

Danielian PS, Muccino D, Rowitch DH, Michael SK, McMahon AP (1998) Modification of gene activity in mouse embryos in utero by a tamoxifen-inducible form of Cre recombinase. Curr Biol 8:1323–1326.

Dause TJ, Kirby ED (2020) Poor Concordance of floxed sequence recombination in single neural stem cells: implications for cell autonomous studies. eNeuro 7:ENEURO.0470-19.2020.

Feil R, Wagner J, Metzger D, Chambon P (1997) Regulation of Cre recombinase activity by mutated estrogen receptor ligand-binding domains. Biochem Biophys Res Commun 237:752–757.

Filardo EJ, Quinn JA, Bland KI, Frackelton AR Jr (2000) Estrogen-induced activation of Erk-1 and Erk-2 requires the G protein-coupled receptor homolog, GPR30, and occurs via trans-activation of the epidermal growth factor receptor through release of HB-EGF. Mol Endocrinol 14:1649–1660.

Gonzalez GA, Hofer MP, Syed YA, Amaral AI, Rundle J, Rahman S, Zhao C, Kotter MRN (2016) Tamoxifen accelerates the repair of demyelinated lesions in the central nervous system. Sci Rep 6:31599.

Hayashi S, McMahon AP (2002) Efficient recombination in diverse tissues by a tamoxifen-inducible form of Cre: a tool for temporally regulated gene activation/inactivation in the mouse. Dev Biol 244:305–318.

Hornsby AKE, Redhead YT, Rees DJ, Ratcliff MSG, Reichenbach A, Wells T, Francis L, Amstalden K, Andrews ZB, Davies JS (2016) Short-term calorie restriction enhances adult hippocampal neurogenesis and remote fear memory in a Ghsr-dependent manner. Psychoneuroendocrinology 63:198–207.

Jorgensen C, Wang Z (2020) Hormonal regulation of mammalian adult neurogenesis: a multifaceted mechanism. Biomolecules 10:1151.

Kiermayer C, Conrad M, Schneider M, Schmidt J, Brielmeier M (2007) Optimization of spatiotemporal gene inactivation in mouse heart by oral application of tamoxifen citrate. Genesis 45:11–16.

Lagace DC, Whitman MC, Noonan MA, Ables JL, DeCarolis NA, Arguello AA, Donovan MH, Fischer SJ, Farnbauch LA, Beech RD, DiLeone RJ, Greer CA, Mandyam CD, Eisch AJ (2007) Dynamic contribution of Nestin-expressing stem cells to adult neurogenesis. J Neurosci 27:12623–12629.

Lee CM, Zhou L, Liu J, Shi J, Geng Y, Liu M, Wang J, Su X, Barad N, Wang J, Sun YE, Lin Q (2020) Single-cell RNA-seq analysis revealed long-lasting adverse effects of tamoxifen on neurogenesis in prenatal and adult brains. Proc Natl Acad Sci U S A 117:19578–19589.

Li W, Wu M, Zhang Y, Wei X, Zang J, Liu Y, Wang Y, Gong C-X, Wei W (2020) Intermittent fasting promotes adult hippocampal neuronal differentiation by activating GSK-3β in 3xTg-AD mice. J Neurochem 155:697–713.

Mazzucco CA, Lieblich SE, Bingham BI, Williamson MA, Viau V, Galea LAM (2006) Both estrogen receptor α and estrogen receptor β agonists enhance cell proliferation in the dentate gyrus of adult female rats. Neuroscience 141:1793–1800.

McAvoy KM, Sahay A (2017) Targeting adult neurogenesis to optimize hippocampal circuits in aging. Neurotherapeutics 14:630–645.

McDonnell DP, Wardell SE (2010) The molecular mechanisms underlying the pharmacological actions of ER modulators: implications for new drug discovery in breast cancer. Curr Opin Pharmacol 10:620–628.

Miller SM, Sahay A (2019) Functions of adult-born neurons in hippocampal memory interference and indexing. Nat Neurosci 22:1565–1575.

Rotheneichner P, Romanelli P, Bieler L, Pagitsch S, Zaunmair P, Kreutzer C, König R, Marschallinger J, Aigner L, Couillard-Després S (2017) Tamoxifen activation of Cre-recombinase has no persisting effects on adult neurogenesis or learning and anxiety. Front Neurosci 11:27.

Semerci F, Maletic-Savatic M (2016) Transgenic mouse models for studying adult neurogenesis. Front Biol (Beijing) 11:151–167.

Srinivas S, Watanabe T, Lin C-S, Tanabe Y, Jessell TM, Costantini F (2001) Cre reporter strains produced by targeted insertion of EYFP and ECFP into the ROSA26 locus. BMC Dev Biol 1:4.

Sun MY, Yetman MJ, Lee TC, Chen Y, Jankowsky JL (2014) Specificity and efficiency of reporter expression in adult neural progenitors vary substantially among nestin-CreER(T2) lines. J Comp Neurol 522:1191–1208.

Toda T, Parylak SL, Linker SB, Gage FH (2019) The role of adult hippocampal neurogenesis in brain health and disease. Mol Psychiatry 24:67–87.

Valny M, Honsa P, Kirdajova D, Kamenik Z, Anderova M (2016) Tamoxifen in the mouse brain: implications for fate-mapping studies using the tamoxifen-inducible Cre-loxP system. Front Cell Neurosci 10:243.

Vivacqua A, Bonofiglio D, Albanito L, Madeo A, Rago V, Carpino A, Musti AM, Picard D, Andò S, Maggiolini M (2006a) 17beta-estradiol, genistein, and 4-hydroxytamoxifen induce the proliferation of thyroid cancer cells through the g protein-coupled receptor GPR30. Mol Pharmacol 70:1414–1423.

Vivacqua A, Bonofiglio D, Recchia AG, Musti AM, Picard D, Andò S, Maggiolini M (2006b) The G protein-coupled receptor GPR30 mediates the proliferative effects induced by 17beta-estradiol and hydroxytamoxifen in endometrial cancer cells. Mol Endocrinol 20:631–646.

Yoshinobu K, Araki M, Morita A, Araki M, Kokuba S, Nakagata N, Araki K (2021) Tamoxifen feeding method is suitable for efficient conditional knockout. Exp Anim 70:91–100.

Zhang Z, Park JW, Ahn IS, Diamante G, Sivakumar N, Arneson D, Yang X, van Veen JE, Correa SM (2021) Estrogen receptor alpha in the brain mediates tamoxifen-induced changes in physiology in mice. Elife 10:e63333.